Mechanistic Studies of Methanol Oxidation to Formaldehyde on Isolated Vanadate Sites Supported on MCM-48

Jason L. Bronkema and Alexis T. Bell*

Chemical Sciences Division, Lawrence Berkeley National Laboratory and Department of Chemical Engineering, University of California, Berkeley, California 94720-1462

Received: August 16, 2006; In Final Form: October 10, 2006

The mechanism of methanol oxidation to formaldehyde catalyzed by isolated vanadate species supported on silica has been investigated by in situ Raman and TPD/TPO experiments. Raman, XANES, and EXAFS were used to characterize the V-MCM-48 sample, prepared with a loading of 0.3 V/nm^2, and it is concluded that the oxidized form of the vanadium is isolated VO_4 units. The VO_4 species consist of one V═O bond and three V−O−Si bonds in a distorted tetrahedral geometry. Methanol reacts reversibly, at a ratio of approximately 1 methanol per V, with one V−O−Si to produce both V−OCH_3/Si−OH and V−OH/Si−OCH_3 group pairs in roughly equivalent concentrations. Formaldehyde is formed from the methyl group of V−OCH_3, most likely by the transfer of one H atom to the V═O bond of the vanadium containing the methoxide group. Formaldehyde is formed in nearly equal concentrations both in the presence and in the absence of gas-phase oxygen. CO and H_2 are produced by the decomposition of CH_2O at higher temperature. In the absence of O_2, Si−OCH_3 groups undergo hydrogenation to form CH_4, and in the presence of O_2, these groups are oxidized to CO_x (x = 1, 2) and H_2O above 650 K. Under steady-state reaction conditions, CH_2O is produced as the dominant product of methanol oxidation at temperatures below 650 K with an apparent activation energy of 23 kcal/mol. Schemes for the product flows during both TPD and TPO experiments, along with proposed surface intermediates, are presented.

Introduction

A central objective in the field of catalysis is to establish relationships between the composition and structure of catalytically active centers and their activity and selectivity. For most heterogeneous catalysts this is a difficult task because of the heterogeneity of active sites, making it nearly impossible to determine the environment of an active site uniquely. For these reasons there has been a growing interest in the preparation and investigation of single-site heterogeneous catalysts.[1] Examples of single site heterogeneous catalysts include single metal oxo units grafted onto the surface of a support,[2] single metal atoms or cations incorporated into the surface of a support,[3] and single crystals that have been uniformly doped to isolate a certain type of atom.[4] By controlling the local structure so that the material is uniform, the active centers are known and structure−reactivity relationships can be more easily determined.

Isolated VO_4 units dispersed on high surface area metal oxides such as TiO_2, SiO_2, and Al_2O_3 have received considerable attention because such catalysts are active for many different reactions, including the partial oxidation of methanol to formaldehyde,[5,6,7] the oxidative dehydrogenation of ethane to ethene,[8] propane to propene,[1] and *n*-butane to maleic anhydride.[9] Because of its inertness relative to other supports, VO_4 units supported on silica are well suited for mechanistic investigations. Moreover, the structure and physical properties of isolated vanadate species supported on silica have been well characterized by UV−visible spectroscopy,[10,11] Raman and infrared spectroscopy,[5,9−11] ^{51}V NMR,[12] XANES,[13] and EXAFS,[14] leading to the conclusion that silica-supported VO_4 species have a distorted tetrahedral geometry containing a single V═O bond and three V−O−Si bonds.

The objective of this study was to investigate the mechanism of methanol oxidation to formaldehyde catalyzed by isolated vanadate species supported on silica. Previous studies have shown that isolated vanadate species are active for this reaction.[5] At lower reaction temperatures CH_2O and water are produced exclusively but with increasing temperature, the yield of CH_2O decreases as CO and CO_2 appear in the products. The formation of CO is believed to be due to the decomposition of CH_2O to CO and H_2, and the formation of CO_2 to the combustion of CO. At temperatures where CH_2O decomposition can occur, the rate of H_2O formation shows an increase over what is expected solely for the formation CH_2O, as additional H_2O is formed via combustion of the H_2 released by CH_2O decomposition. Studies of the reaction kinetics show that at low surface concentrations of adsorbed methanol, the rate of formaldehyde formation is first order in methanol and the reaction is zero order in oxygen when oxygen is present in excess and the vanadia sites are fully oxidized.[15] A mechanism for the reaction has been proposed to interpret the observed kinetics. Methanol adsorption is envisioned to occur by reversible reaction with V−O−Si bonds, leading to the formation of both V−OCH_3/Si−OH and V−OH/Si−OCH_3 pairs. The rate-limiting step is proposed to be the release of an H atom from V−OCH_3, possibly to the V═O bond, and desorption of CH_2O. Theoretical studies support the mechanism suggested on the basis of experimental observations and show that, as found experimentally, roughly half of the methanol adsorbs in such a way as to form Si−OCH_3 and V−OH groups.[16]

In this paper, we explore the mechanism for the partial oxidation of methanol to formaldehyde on V/MCM-48. Raman

* Author to whom correspondence should be addressed. E-mail: alexbell@berkeley.edu.

10.1021/jp0653149 CCC: $37.00
Published on Web 11/30/2006

spectroscopy, XANES, and EXAFS were used to characterize the catalyst, and in situ Raman spectra acquired during temperature-programmed desorption (TPD), temperature-programmed oxidation (TPO), and temperature-programmed reaction (TPRx) were used to determine reaction intermediates leading to the formation of formaldehyde as well as other products observed in the gas phase. These studies show that while $V-OCH_3$ groups are the exclusive source of formaldehyde, $Si-OCH_3$ groups contribute to the formation of CO and CO_2.

Experimental Methods

A high-surface area mesoporous silica, MCM-48, was prepared following the procedures reported in the literature.[17,18] Gemini 16-12-16, the surfactant required for the synthesis of MCM-48, was prepared as follows.[19] Stoichiometric amounts of 1,12-dibromododecane and *N*,*N*-dimethylhexadecylamine were dissolved in acetone and refluxed under stirring at 340 K for 24 h. After cooling to 295 K, the white crystals that precipitated were collected by vacuum filtration and washed with a minimum amount of ice cold acetone. The preparation of MCM-48 was initiated by dissolving the Gemini surfactant and sodium hydroxide in deionized water. After vigorous stirring for at least 30 min, tetraethylorthosilicate (TEOS) was added and the mixture was stirred for 2 h. The molar ratio of the reactants was GEM:NaOH:H_2O:TEOS (0.06:0.6:150:1). This solution was transferred to a Teflon-lined autoclave and heated at 373 K for 5 days. After vacuum filtration, the collected solid was dissolved in 20 g of H_2O per gram of collected product and heated in the autoclave reactor at 373 K for 4 additional days.[5] The MCM-48 was obtained by vacuum filtration after washing with water. The sample was heated in flowing air from 298 to 823 K at 2 deg min^{-1} and then held at 823 K for 5 h.

Vanadium oxide was deposited onto MCM-48 by chemical vapor deposition.[20] A calculated amount of vanadium acetylacetonate [$VO(acac)_2$] and MCM-48 were mixed in a mortar and pestle and placed inside a quartz reactor. The mixture was heated to 513 K at 5 deg min^{-1} in N_2 flowing at 30 cm^3 min^{-1} and then held at this temperature for 3 h to ensure complete reaction. The gas flow was then changed to zero-grade air at 100 cm^3 min^{-1} and the material was calcined at 773 K for 17 h. The weight loading of V was determined by ICP.

The BET surface area of the sample was measured with an Autosorb-1 instrument. Prior to carrying out N_2 adsorption/desorption measurements each sample (25 mg) was outgassed for 2 h at 393 K. The five-point BET method was used to calculate the surface area while the pore size distribution and the total pore volume were calculated from the desorption isotherm by using the method of Barrett, Joyner, and Halenda (BJH).[21]

The XRD pattern was obtained by using a Siemens D5000 diffractometer. Diffraction measurements were made with Cu Kα radiation over the 2θ interval of 2−5° with a step size of 0.015° and a time per step of 15 s. The sample was placed in a sample holder and smoothed to a flat surface with a spatula.

Raman spectra were recorded with a Kaiser Optical HoloLab series 5000 Raman spectrometer equipped with a Nd:YAG laser that is frequency-doubled to 532 nm. The laser was operated at a power level of 25 mW measured at the sample with a power meter. A Princeton Instruments TEA/CCD detector was operated at −40 °C. Spectra were recorded with a resolution of 2 cm^{-1}. Samples (approximately 25 mg each) were pressed into pellets at 5000 psi and placed within a rotary quartz Raman cell. The samples were rotated at 100 rpm during the measurements to reduce the effects of sample heating by the laser.

Pulsed-adsorption of methanol was performed to determine the amount of methanol adsorbed on MCM-48 and V/MCM-48. For these experiments, ~25 mg of catalyst was placed into a quartz microreactor. The reactor was flushed with UHP He and then heated to 323 K. Methanol was introduced by flowing UHP He through a methanol-filled bubbler maintained at 293 K. The methanol/He mixture was passed through a six-way valve to which was attached a 0.49 cm^3 dosing volume held at 338 K. Under these conditions, the amount of methanol in each pulse was 2.28 μmol. The exit stream from the microreactor was monitored by a mass spectrometer to quantify the methanol leaving the reactor during each pulse. Pulses of methanol were supplied to the reactor until three successive pulses of equal size were observed. The total amount of methanol adsorbed, N_{MeOH}, was calculated by the equation:

$$N_{MeOH} = N^0_{MeOH}(nA_{max} - \sum_{i=1}^{n} A_i)/nA_{max} \quad (1)$$

where N^0_{MeOH} is the amount of methanol in each pulse, n is the total number of pulses, A_{max} is the average area of the three successive pulses measured at the point of adsorbent saturation, and A_i is the area of the ith pulse of methanol observed by the mass spectrum.

For the Raman and TPD/TPO experiments, methanol adsorption was carried out using a mixture of 4% methanol in helium flowing at 30 cm^3 min^{-1}. A catalyst pellet weighing ~25 mg was exposed to the methanol-containing gas at 323 K for 3 min. A short exposure time was used to minimize the loss of vanadium from the catalyst (see below). Following adsorption, the Raman cell was purged with a flow of 100 cm^3 min^{-1} of He for at least 45 min to reduce the amount of residual methanol in the gas phase. For TPD experiments the samples were then heated in 30 cm^3 min^{-1} flow of He, whereas for TPO experiments, the samples were heated in 30 cm^3 min^{-1} flow of 5% O_2/He. For both types of experiment, the temperature was ramped from 323 to 773 K at 4 deg/min. Raman spectra were collected every 75 s to obtain a scan every 5 K. The effluent from the Raman cell was analyzed by an MKS Mini-Lab quadrupole mass spectrometer. Data were collected for 27 masses every 7.5 s. Response factors and fragmentation patterns were determined for H_2, H_2O, O_2, CO, CO_2, CH_3OH, CH_2O, and CH_4 relative to the He signal, which was used as an internal standard, and the values were adjusted to account for the isotopic abundance of both carbon and oxygen. Because the fragmentation pattern of methanol, formaldehyde, oxygen, and carbon monoxide produces overlapping peaks in the range of m/e 28−33, a matrix deconvolution procedure was used to quantify the gas-phase contributions of each species. After analysis, the data were smoothed by using adjacent averaging of 15 points.

X-ray absorption (XAS) measurements were performed at the Stanford Synchrotron Radiation Laboratory (SSRL) on beam lines 2−3 and 4−3 and at the National Synchrotron Light Source (NSLS) on beam line X11A. The measurements were performed at the vanadium K-edge. The edge energy for each sample was determined as the first inflection point of the main peak in the spectrum, and the edge energy of the vanadium foil was set to 5465 eV. The optimal sample amount was calculated based upon the weight fraction of all atomic species to obtain an absorbance of ~2.5, with boron nitride added if necessary to make a stable pellet. Samples were placed in a controlled-atmosphere cell that allowed for heating up to 823 K in the presence of flowing gas.[22] UHP He and 10% O_2 in He were used in these experiments to pretreat the catalyst samples before the XAS

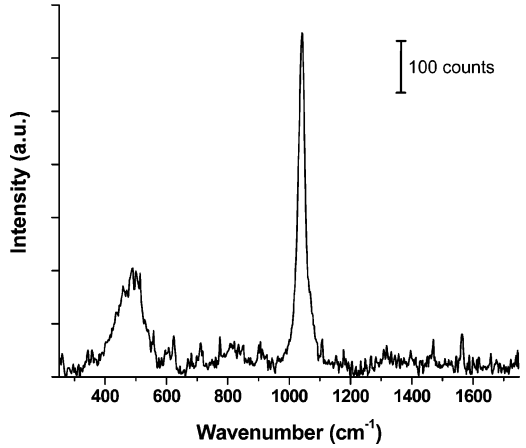

Figure 1. Raman spectrum of 3.4V/MCM-48 after dehydration in dry air at 773 K for 2 h.

measurement. After the pretreatment was completed, the cell was evacuated to 6×10^{-4} Pa and cooled to 77 K before the XAS data were collected. For in situ XANES measurements, scans were made approximately every 7 min at reaction temperature and under gas flow.

The EXAFS portion of the XAS data was analyzed to determine the local coordination around each vanadium atom. The software program IFEFFIT, along with its complementary GUIs Athena and Artemis, were used for the data analysis.[23,24] First, a linear preedge was subtracted from the data, fit to the range of −150 to −75 eV relative to the edge energy. Then a quadratic polynomial fit to the range of 150 to 850 eV for EXAFS and 100 to 300 eV for in situ XANES, both relative to the edge energy, was used to normalize the data. A cubic spline was fit to the normalized data from 2 to 16 $Å^{-1}$ to remove the background absorption and minimize the signal in *R* space below 1 Å. These data were then Fourier transformed over the *k* range of 3.2 to 11.6 by using the Kaiser−Bessel window functions with a d*k* of 1 and a *k* weight of 3. The EXAFS fits were performed in *R* space, with the background fit from 0 to 1 Å and the data fit from 1 to 2.2 Å. The value for S_0^2, determined by performing a fit to vanadium foil, used in the EXAFS analysis was 0.7.

Results

Catalyst Characterization. The surface area of the MCM-48 sample was 1370 m^2/g and the unit cell parameter was 74.2 Å. The total pore volume was 0.86 cm^2/g and the average pore diameter was 19.6 Å. All of these characteristics lie within the range of values reported previously.[5,17,18] The vanadium loading of the sample was measured to be 3.43 wt % V. This corresponds to a surface density of 0.30 V/nm^2, which is well below the maximum surface coverage of isolated vanadium on silica supports of approximately 2 V/nm^2, beyond which isolated vanadate groups begin to form polyvanadate species and V_2O_5 crystallites.[25]

Figure 1 shows the Raman spectra for 3.4V/MCM-48 after dehydration in synthetic air at 773 K for 2 h. The large band at 1035 cm^{-1} has been attributed to a symmetric stretch of V═O in isolated VO_4 units on the silica.[26] No peaks were observed at 995, 704, 529, 288, and 147 cm^{-1} indicative of V_2O_5 formation, suggesting that the calcined sample consists exclusively of isolated vanadate sites.[8,26] The broad feature centered around 480 cm^{-1} is representative of D1 defects in the surface of the silica matrix of MCM-48.[27]

X-ray absorption experiments were also performed to identify the oxidation state and local structure of the vanadium centers

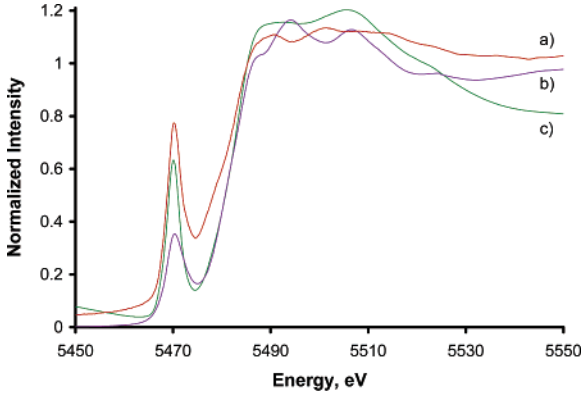

Figure 2. Normalized XANES spectra of (a) $NaVO_3$, (b) V_2O_5, and (c) 3.4V/MCM-48.

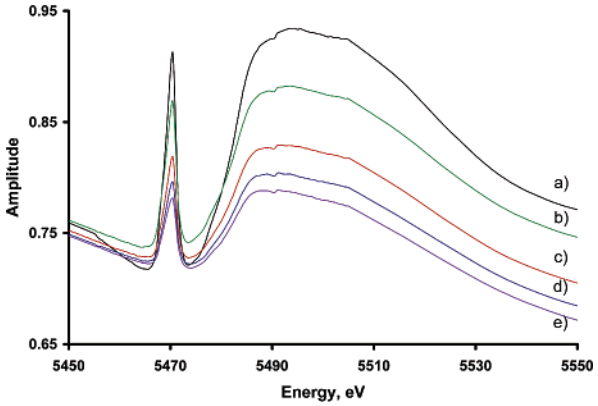

Figure 3. XANES spectra of 3.4V/MCM-48 during addition of 40 cm^3 min^{-1} of 4% MeOH/He at 373 K: (a) initial, (b) 7 min, (c) 14 min, (d) 21 min, and (e) 28 min.

dispersed on the MCM-48. Figure 2 shows the normalized XANES spectrum of 3.4V/MCM-48 after calcination and XANES spectra for $NaVO_3$ and V_2O_5. For the calcined 3.4V/MCM-48, the edge energy was 5484.0 eV. This value lies between the edge energies for V^{5+} in $NaVO_3$ at 5483.5 eV and V_2O_5 at 5484.8 eV, strongly suggesting that after calcination the oxidation state of the 3.4V/MCM-48 is +5.

The V in $NaVO_3$ has tetrahedral symmetry, whereas the V in V_2O_5 has square planar or distorted octahedral symmetry. The size of the preedge peak at 5470 eV can be used to obtain information about the coordination of the vanadium atom if the standards and samples have the same formal oxidation state and the same ligands in the first coordination shell. This peak is attributed to electron transitions from the vanadium 1s to 3d level,[28] which are spin forbidden and therefore should be weak. However, when the geometry around the vanadium atom becomes noncentrosymmetric, mixing between the oxygen 2p and the vanadium 3d levels can occur, leading to an increase in the observed intensity. This means that a purely octahedral geometry will have almost no preedge feature, whereas tetrahedrally coordinated V will have a large preedge feature. On the basis of a comparison to the geometry of the standards, the calcined 3.4V/MCM-48 has a distorted tetrahedral geometry similar to that of $NaVO_3$.

An in situ XANES experiment was performed to determine how the local structure of the vanadium changes upon the adsorption of methanol. Figure 3 shows the data during the addition of 4% methanol in UHP helium at 373 K. The overall intensity of both the main edge and the preedge feature decrease with time. On the basis of the decrease in intensity of the edge step, 68% of the vanadium present originally was lost during

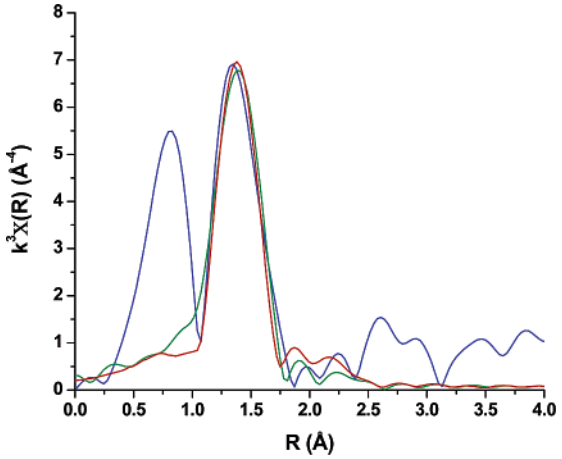

Figure 4. *R*-space plot of 3.4V/MCM-48 along with curves for each fit. The experimental data are shown in blue, the fit to the data with CN as a free parameter is shown in red, and the fit to the date with fixed CN is shown in green. The artifact peak appearing at about 0.7 Å was subtracted from the data prior to fitting it (see text).

the 28 min exposure to methanol. Attempts to calcine the catalyst at 773 K in 10% O_2/He afterward did not recover the signal intensity. The observed loss in the intensity of the XANES signal is attributable to a loss of vanadium from the surface of the materials, most likely due to the formation of a volatile vanadium methoxide species. In a separate experiment, the sample was exposed to 9% methanol in He at 373 K. Over the course of 12 h the content of V declined from 5.2% to 0.9% and a greenish deposit was formed at the exit from the reactor. A similar phenomenon has been reported for silica supported molybdena upon exposure to methanol.[29] In view of these experiments, exposure of the VO_x/SiO_2 sample used for the present work was limited to 2.5 min at 373 K.

Figure 4 shows two large peaks in the non-phase-corrected *R*-space plot of the EXAFS data. The first peak at 0.7 Å is a phantom peak mainly due to oscillations in the background that are not completely removed by the cubic spline. The majority of this peak is removed with a background fit and does not correspond to a physical coordination shell around the vanadium atom. The other large peak at approximately 1.3 Å is in the same position as the first oxygen shell seen in the other vanadium oxide compounds, and it is fit to two vanadium−oxygen shells, one for a vanadium oxygen double bond (V═O) and the other for vanadium oxygen single bonds (V−O). The atomic coordinates given by Khaliullin and Bell,[16] obtained from a DFT calculation of an isolated vanadate species bonded to silica, were used as the basis for the FEFF calculation.[30] The VO_4 cluster in this model contains one V═O bond with a bond length of 1.59 Å and three V−O bonds with bond lengths of 1.77 Å. Table 1 shows that the optimized values for the lengths of the V═O and V−O bonds are within 0.01 and 0.03 Å of those predicted from DFT calculations; however, the coordination numbers, especially for the V═O shell, are lower than expected. This is most likely due to a slight loss of intensity due to destructive interference between the two oxygen shells. Table 1 also shows that the fits performed when the coordination numbers were fixed at 1 and 3 are similar in quality to those in which the coordination number was allowed to change. The statistical error as shown by the larger *R* factor is only slightly larger in the latter case. As can be seen by Figure 4, the fits look very similar when the coordination number is fixed or varied.

Another thing to notice in the EXAFS data is the absence of a peak between 2.2 and 2.8 Å, which is the region where second shell vanadium contributions are observed in V_2O_5 and other bulk vanadium oxides,[31] as well as the region were V−V interactions in dimeric or polymeric VO_4 would occur. Small features are observed in this area due to the spectral leakage of performing a finite Fourier transform, but no peak could be fit successfully to V−V scattering with V_2O_5 as the model, while allowing both the coordination number and bond distance to vary during the fit. This is a strong indication that the sample consists predominantly of isolated VO_4 tetrahedra bonded to the surface of MCM-48.

TPD and TPO of Methanol Adsorbed on MCM-48. The Raman spectrum of MCM-48 is shown in Figure 5. Broad bands appearing at 480 and 610 cm^{-1} are seen prior to the exposure of the sample to methanol, which are attributable to D1 and D2 surface defects in MCM-48.[27] The band at 3740 cm^{-1} is assignable to O−H stretch vibrations of silanol groups on the surface of MCM-48.[32] Upon addition of methanol, a number of new features are observed in the spectrum. In the presence of gas-phase methanol, two large peaks centered at 2848 and 2951 cm^{-1} are observed together with a peak at 1000 cm^{-1}. These peaks are due to the symmetric and asymmetric C−H stretching virbrations and the C−O stretching vibration of weakly adsorbed methanol interacting with surface silanol groups. This interpretation is supported by the observed loss of intensity in the silanol band at 3740 cm^{-1}. After the He purge all three peaks disappear, and two small bands at 2861 and 2961 cm^{-1} are observed, attributable to C−H stretching vibrations of $Si-OCH_3$ groups. A small feature also appears at 1460 cm^{-1}, attributable to C−H bending vibrations in $Si-OCH_3$ groups.[32] The small peak at 1560 cm^{-1} present in all scans is due to gas-phase oxygen, which is present between the focusing optics and the Raman cell, but it is not in contact with the sample. The area of the silanol band decreases following the adsorption of methanol and the purge of gas-phase methanol, suggesting that methanol may have reacted with some of the silanol groups.

Raman spectra recorded during the temperature-programmed desorption of methanol adsorbed on MCM-48 are presented in Figure 6 and the compositions of the species present in the gas phase are presented in Figure 7. Figure 6 shows that the intensity of the $Si-OCH_3$ bands at 2861 and 2961 cm^{-1} decreases monotonically as the temperature is increased, but some of these species still remain at 673 K. Figure 7 shows that the only gas-phase species detected leaving the surface is methanol. Methanol desorption begins above 350 K, reaches a maximum at about 500 K, and then gradually diminishes with increasing temperature. The total amount of methanol desorbed (see Table 2) corresponds to 2.5 μmol, or 0.06 CH_3OH/nm^2, and is in good agreement with the amount of adsorbed methanol determined by pulsed adsorption. The retention of nearly half of the original compliment of $Si-OCH_3$ groups at 773 K indicates that a significant portion of the methanol adsorbed at 323 K remains on the silica surface after TPD up to 773 K. This finding is consistent with previous work, which showed that $Si-OCH_3$ groups can be stable up to 900 K.[32]

Raman spectra recorded during the TPO of methanol adsorbed on MCM-48 are shown in Figure 8 and the composition of gas-phase species produced during this process is presented in Figure 9. Comparison of Figures 6 and 8 reveals that the decreases in the intensity of the Raman bands for $Si-OCH_3$ groups are similar in TPD and TPO, but above 623 K, the loss of these groups during TPO is much more significant. Figure 9 shows that up to 600 K the principal component seen in the gas phase is methanol. This observation is similar to what was observed during TPD. However, above 600 K, sharp peaks are observed

TABLE 1: Summary of EXAFS Fitting Results for 3.4V/MCM-48 after Calcination in Oxygen at 773 K[a]

	shell	CN	distance (Å)	E_0 (eV)	σ^2 ($\times 10^3$)	R factor
3.4V/MCM-48	V═**O**	0.5 ± 0.8	1.59 ± 0.09	0.5 ± 8.2	1.4 ± 4.7	0.033
	V−**O**	2.7 ± 1.6	1.80 ± 0.03			
3.4V/MCM-48	V═O	1	1.58 ± 0.03	−4.0 ± 3.7	1.4 ± 1.2	0.045
	V−**O**	3	1.79 ± 0.02			

[a] The first set of entries give the results obtained when the coordination numbers are allowed to vary and the second set of entries give the results when the coordination numbers are set at 1 and 3.

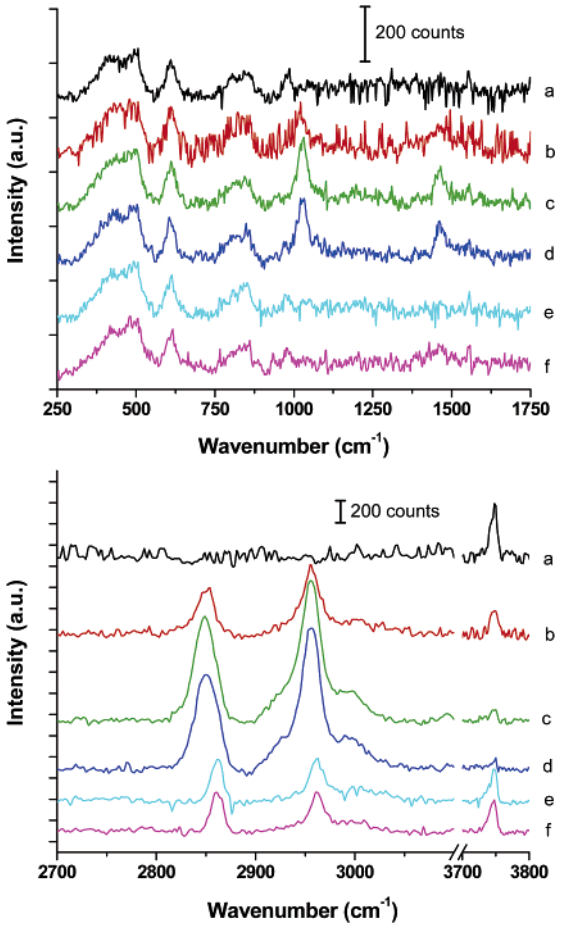

Figure 5. Low and high wavenumber Raman spectra of MCM-48 during methanol adsorption at 323 K and subsequent He purge: (a) initial spectrum in He, (b) after 1 min in methanol, (c) after 2.5 min in methanol, (d) after purging in He for 1 min, (e) after purging in He for 3.5 min, and (f) after purging in He for 45 min.

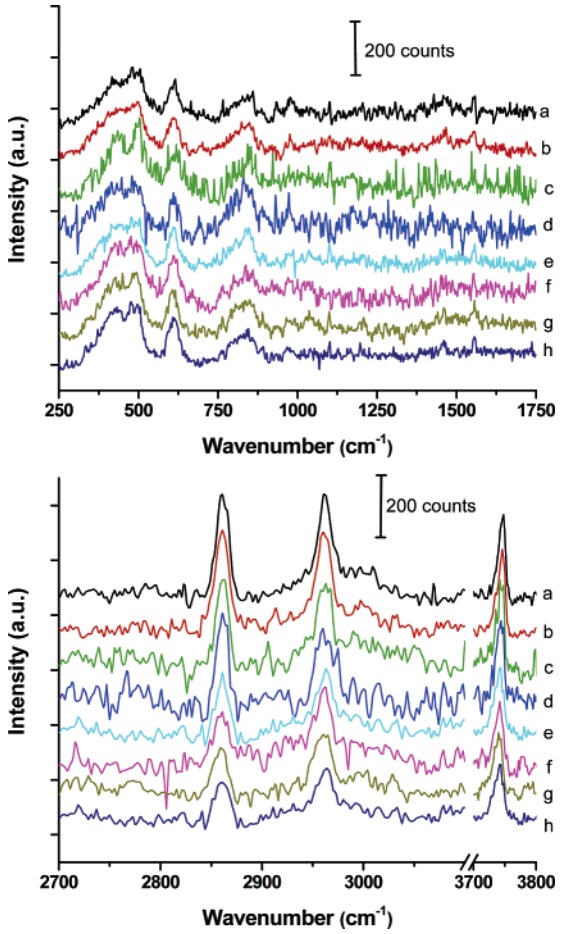

Figure 6. Low and high wavenumber Raman spectra of MCM-48 taken during TPD of adsorbed methanol: (a) 323, (b) 373, (c) 423, (d) 473, (e) 523, (f) 573, (g) 623, and (h) 673 K. Flow rate of He was 30 cm^3 min^{-1}.

for CO_2 and H_2O, which reach their maxima at about 650 K. The ratio of H_2O to CO_2 formed is approximately 2:1. The amount of carbon removed from the surface of MCM-48 during TPO as CH_3OH (2.4 μmol) and CO_2 (1.1 μmol) is 3.5 μmol. These results taken together with those for the TPD of adsorbed methanol suggest that 69% of the methanol adsorbed at 323 K can be desorbed as CH_3OH at temperatures up to 773 K, whereas 31% can only be removed by combustion. Of further note is that the amount of adsorbed methanol determined by pulsed adsorption agrees reasonably well with the total amount of carbon removed during TPO.

TPD and TPO of Methanol Adsorbed on 3.4V/MCM-48. Figure 10 shows Raman spectra taken during the adsorption of methanol on 3.4/MCM-48. The spectrum taken prior to methanol exposure is identical with that shown in Figure 1, and exhibits bands at 1035 cm^{-1} for the V═O stretching vibrations of isolated vanadate species and at 200−500 cm^{-1} for D1 surface defects in MCM-48. Upon adsorption of methanol, a new band appears at 1070 cm^{-1}. This band has been previously attributed to the C−O bending mode in V−OCH_3.[33] New bands are also seen at 2830, 2861, 2930, and 2961 cm^{-1} and at 1450 and 1460 cm^{-1}. The peaks at 1460, 2861, and 2961 cm^{-1} were previously observed on the MCM-48, and have been assigned to Si−OCH_3 groups. Consequently, the features at 1450, 2830, and 2930 cm^{-1} are assigned to the bending and stretching modes of V−OCH_3 groups formed by the addition of CH_3OH across V−O−Si bonds.[34] It is observed that the bands for V−OCH_3 increase more rapidly in the first scan after methanol addition, and then the ratio of V−OCH_3 to Si−OCH_3 bands equilibrate on the surface. This pattern suggests that the formation of V−OCH_3/Si−OH pairs may occur more rapidly than the formation of V−OH/Si−OCH_3 pairs when CH_3OH adds across the V−O−Si bonds. The loss of the silanol peak at 3740 cm^{-1} during methanol addition suggests that some of the adsorbed methanol interacts with Si−OH groups on the surface of MCM-48. A band at 670 cm^{-1} appears during the addition of methanol and is almost completely removed during the helium purge. This band is most likely due to methanol very weakly adsorbed on vanadium. The residual band after the He purge is likely due

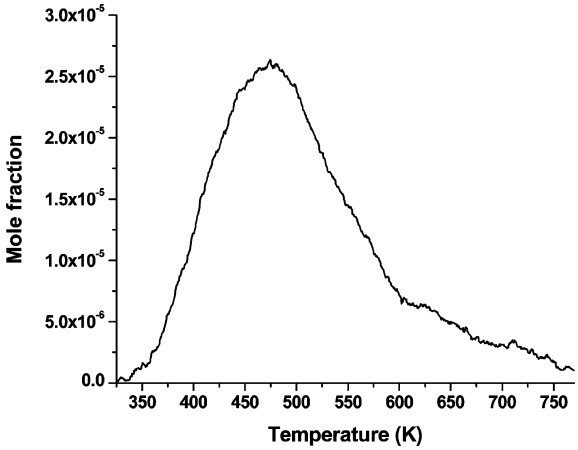

Figure 7. Gas-phase concentration of methanol during TPD of methanol adsorbed on MCM-48. Flow rate of He is 30 cm^3 min^{-1}.

to a V−O stretch due to surface V−OCH_3 groups.[33] A very small band at 1130 cm^{-1} is also observed on the sample, which is likely due to the C−O stretching mode of methanol in the gas phase because this peak also decreases rapidly during the He purge and is removed completely after 5 min.[35]

Raman spectra recorded during the TPD of methanol adsorbed on 3.4V/MCM-48 are presented in Figure 11 and the composition of the gas phase is presented in Figure 12. With increasing temperature, the bands for V−OCH_3 groups diminish more rapidly than those for Si−OCH_3 groups. Evidence for the loss of V−OCH_3 groups can also be seen in the decrease in intensity of the band at 1070 cm^{-1}. Figure 12 shows that as the temperature increases initially, a broad peak appears for the desorption of methanol. This peak is similar in shape and position to that observed on MCM-48, but is about 2.5 times larger in area. A peak for formaldehyde appears at 350 K and reaches a maximum at about 590 K. This product is formed from the methanol associated with the vanadium centers, since formaldehyde was not observed during the TPD of methanol adsorbed on MCM-48. Above 550 K, three species are desorbed from the surface: methane, carbon monoxide, and hydrogen. These products were also not observed during the TPD of methanol adsorbed on MCM-48, and hence are attributable to the presence of V. It is also interesting to observe that in contrast to what is observed for MCM-48, the residuum of Si−OCH_3 groups is much smaller for 3.4V/MCM-48 after TPD to 773 K. Of further note is the observation that the V═O band at 1035 cm^{-1} is only 30% of the original intensity at the end of the TPD experiment. This is very likely due to a partial reduction of the sample during the course of TPD, which both removes the V═O and results in a shallower sampling depth in the catalyst pellet because of a higher optical absorbance.[36] The intensity of the band at 1035 cm^{-1} can be restored completely, though, upon reoxidation of the 3.4V/MCM-48 sample.

Raman spectra recorded during the TPO of methanol adsorbed on 3.4V/MCM-48 are presented in Figure 13 and the composition of the gas phase is presented in Figure 14. Figure 13 shows that the loss of V−OCH_3 occurs at lower temperatures than during TPD (compare with Figure 11). It is also evident that the intensity of the V═O band at 1035 cm^{-1} observed at 773 K is more intense than that observed at the same temperature during a TPD experiment, indicating that the reoxidation of reduced VO_x species occurs during TPO. Another difference between the TPO and TPD experiments is the reappearance of the Si−OH band at 3740 cm^{-1} at the end of the TPO experiment, but not at the end of the TPD experiment. Figure 14 shows that the formation of formaldehyde begins at 325 K and reaches a maximum at about 585 K. This peak is larger than that observed in the TPD experiment but has a similar profile and maximum peak temperature. There is also a CO desorption peak centered at 625 K that is most likely due to the decomposition of formaldehyde to CO and H_2. At 650 K peaks are evident in the formation of CO_2 and H_2O similar to those observed during the TPO of methanol adsorbed on MCM-48. It is interesting to note that the formation of H_2O occurs already at 325 K and exhibits a broad peak at 375 K. It is also noted that both the H_2O and the CO_2 traces exhibit a broad feature, which reaches a maximum at about 750 K. The amounts of each gas-phase product formed are listed in Table 2 together with the total amounts of carbon and hydrogen contained in these products. The total amount of carbon released in various products corresponds to 20.7 μmol, which is comparable to the amount of V in the sample, 24 μmol, and slightly less than the total amount of carbon released as products during the TPD of methanol adsorbed on 3.4V/MCM-48, 23.1 μmol. For both TPO and TPD, though, the ratio of H to C in the products is close to 3. While the amounts of CH_3OH, CH_2O, and CO produced during TPO and TPD are similar, the remaining products formed during TPO are CO_2 and H_2O as opposed to CH_4 and H_2, and a small amount of CO_2, during TPD.

The results of TPRx are illustrated in Figures 15 and 16. A mixture of 5% MeOH/7.5% O_2/balance He was flowed over the catalyst and the temperature was ramped from 473 to 773 K. The Raman spectra recorded at reaction temperatures between 473 and 773 K, shown in Figure 15, are very similar to those shown in Figure 13 for the TPO of adsorbed methanol taken over the same temperature range. Figure 16 shows that the formation of both formaldehyde and water is observed starting at 530 K. The formaldehyde concentration reaches a maximum at a temperature of 700 K, and then decreases due to the decomposition of CH_2O to CO and H_2 and the subsequent oxidation of H_2 to H_2O. The water signal increases with temperature as methanol is converted to formaldehyde, which is further decomposed to produce another H_2O molecule per methanol. The signal for CO increases in a manner similar to that of the H_2O signal. A spike in both the H_2O and CO produced occurs at 673 K at the same time that a small drop in the O_2 signal is observed. This likely occurs due to the oxidation of residual surface methoxy groups on the silica, as seen in both the MCM-48 and 3.4V/MCM-48 TPO experiments above.

Discussion

At 323 K, the amount of methanol adsorbed on MCM-48 is considerably less than the concentration of Si−OH groups, which is estimated to be ~1/nm^2. Raman spectroscopy shows that methanol adsorption on MCM-48 produces Si−OCH_3 groups. During TPD most of these species desorb as methanol; however, about a third of the originally adsorbed methanol remains as Si−OCH_3 following TPD up to 773 K. The reversibility of a large part of the adsorbed methanol suggests that the reaction CH_3OH + Si−O−Si → Si−OCH_3 + Si−OH occurs upon adsorption, and the reverse of this reaction occurs upon desorption. Consistent with this interpretation it is noted that the H/C ratio of the products observed during TPD is 4. The data in Table 2 indicate that the amount of methanol adsorbed in this fashion corresponds to 0.04 CH_3OH/nm^2. The Si−OCH_3 groups that are not removed during TPD are removed during TPO at temperatures above 600 K (see Figure 9). It is hypothesized that these Si−OCH_3 groups are formed by the reaction CH_3OH + Si−OH → Si−OCH_3 + H_2O. Evidently, these Si−OCH_3 groups cannot form methanol since they are

TABLE 2: Total Amounts of Each Product Released into the Gas Phase during TPD and TPO of Methanol Adsorbed on MCM-48 and 3.4V/MCM-48[a]

		CH_3OH	CH_2O	CO	CO_2	H_2O	H_2	CH_4	total C	total H	MeOH dsorbed
MCM-48	TPD	2.5	0.0	0.0	0.0	0.0	0.0	0.0	2.5	9.8	2.4
MCM-48	TPO	2.4	0.0	0.0	1.1	2.3	0.0	0.0	3.5	14.1	2.6
V-MCM-48	TPD	6.7	4.7	4.1	0.5	0.0	2.1	7.1	23.1	68.8	26.1
V-MCM-48	TPO	5.6	5.1	4.9	5.2	15.2	0.0	0.0	20.7	63.0	20.1

[a] Also shown is the total amount of carbon and hydrogen removed from the surface. The last column gives the amount of methanol adsorbed determined by pulsed adsorption. All quantities are in μmol.

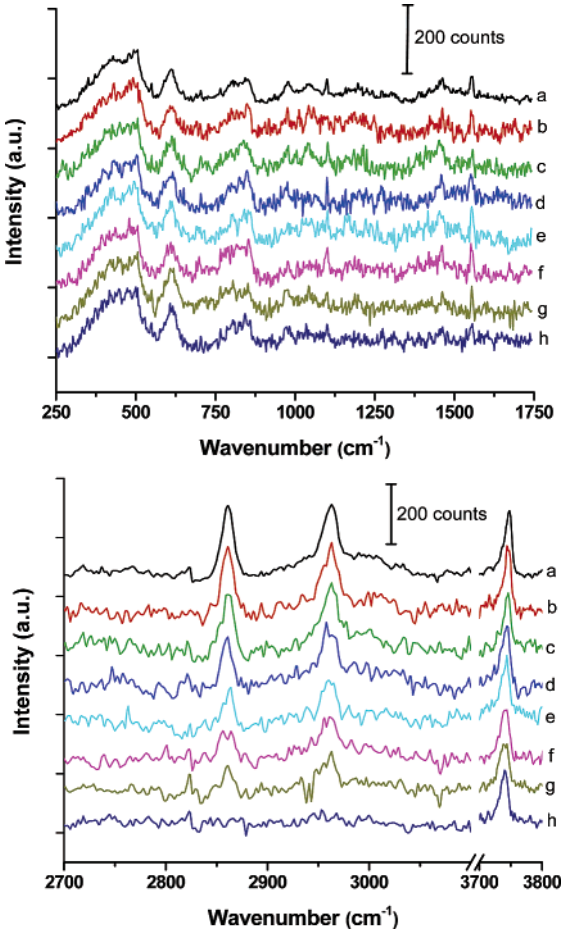

Figure 8. Low and high wavenumber Raman spectra of MCM-48 taken during TPO of adsorbed methanol: (a) 323, (b) 373, (c) 423, (d) 473, (e) 523, (f) 573, (g) 623, and (h) 673 K. Flow rate of 5% O_2/He is 30 cm^3 min^{-1}.

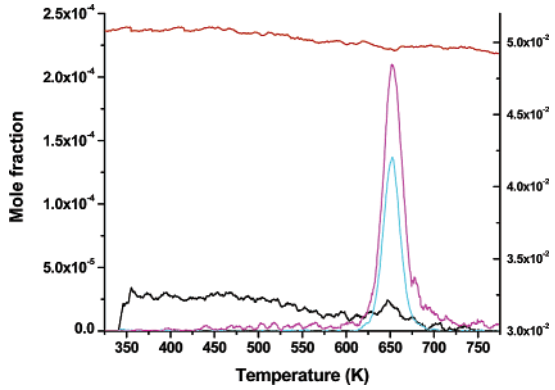

Figure 9. Gas-phase concentrations observed during TPO of methanol adsorbed on MCM-48. Flow rate of 5% O_2/He is 30 cm^3 min^{-1}. Left axis: methanol, black; water, pink; carbon dioxide, light blue. Right axis: oxygen, red.

not proximate to Si−OH groups, but in the presence of O_2 these groups can undergo combustion above 600 K via the reaction $Si{-}OCH_3 + {}^3/_2O_2 \rightarrow Si{-}OH + CO_2 + H_2O$.

The amount of methanol adsorbed by 3.4V/MCM-48 is nearly an order of magnitude higher than that adsorbed by MCM-48. As seen in the Raman spectra presented in Figure 10, both $V{-}OCH_3$ and $Si{-}OCH_3$ species are formed, with the former being present in somewhat higher concentration. This suggests that the heats of methanol adsorption for the two modes of adsorption are comparable, in good agreement with theoretical prediction.[16] Table 2 also shows that the amounts of adsorbed methanol deduced from both pulsed adsorption and TPD/TPO experiments are in good agreement, indicating that virtually all of the adsorbed methanol is released during a TPD and TPO experiment.

The TPD spectrum observed for methanol adsorbed on 3.4V/MCM-48 (see Figure 12) is qualitatively similar to those reported by Feng and Vohs[37] for highly dispersed vanadia on silica, with the exception that in the present study CH_4 and H_2 are observed in the effluent products in addition to CH_3OH, CH_2O, and CO. Also in contrast to the observations of Feng and Vohs, no evidence was found in the present study for the agglomeration of VO_4 units into polyvanadates or V_2O_5 at the end of TPD. Methanol desorption occurs already at 350 K and continues up to 700 K. The formation of CH_2O also begins at 350 K, accelerates significantly above 500 K, and reaches a peak at about 575 K. The signals for CH_4, CO, and H_2 appear above 550 K and reach a maximum at about 600 K.

The origin of the gas-phase products observed during the TPD of methanol adsorbed on 3.4V/MCM-48 and the distribution of these products can be rationalized by using the scheme shown in Figure 17. The adsorption of methanol produces both $V{-}OCH_3/Si{-}OH$ and $V{-}OH/Si{-}OCH_3$ group pairs. During TPD, each pair of species can recombine to release methanol and reform the V−O−Si bond that was cleaved upon methanol adsorption. Consistent with this interpretation, the Raman spectra in Figure 11 show a decrease in surface concentrations of both $V{-}OCH_3$ and $Si{-}OCH_3$ groups. The distribution of $V{-}OCH_3/Si{-}OH$ versus $V{-}OH/Si{-}OCH_3$ pairs is defined under the assumption that CH_2O and products produced by the decomposition of CH_2O derive from $V{-}OCH_3/Si{-}OH$. CH_2O is taken to be formed by the transfer of an H atom from the $V{-}OCH_3$ group to the V═O bond of the vanadyl methoxide structure consistent with recent theoretical studies.[38] As the temperature increases, a portion of the CH_2O released undergoes decomposition to form CO and H_2. Most of the CO enters into the gas phase and only a small fraction is combusted to CO_2. A portion of the H_2 produced by the decomposition of CH_2O is released to the gas phase and the balance is assumed to react with the $Si{-}OCH_3$ groups to form CH_4 and Si−OH groups. The balance of the CH_4 observed is thought to come from the reaction of the hydrogen in V−OH groups with $Si{-}OCH_3$. The companion product in this case is a vanadylsilicoperoxide species. While such species do not have an experimental precedent, recent DFT

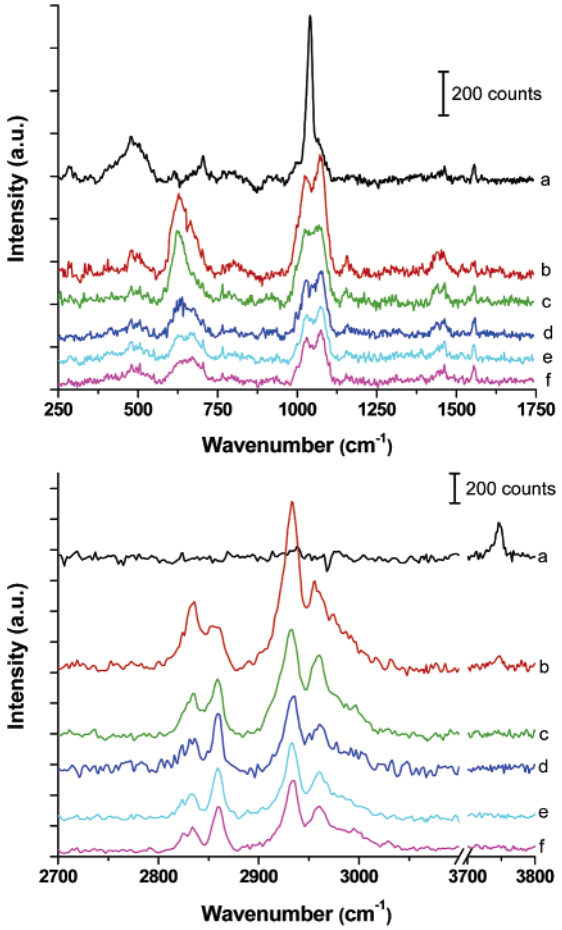

Figure 10. Low and high wavenumber Raman spectra of 3.4V/MCM-48 taken during methanol adsorption at 323 K and subsequent He purge: (a) initial spectrum in He, (b) after 1 min in methanol, (c) after 2.5 min in methanol, (d) after He purge for 1 min, (e) after He purge for 3.5 min, and (f) after He purge for 45 min.

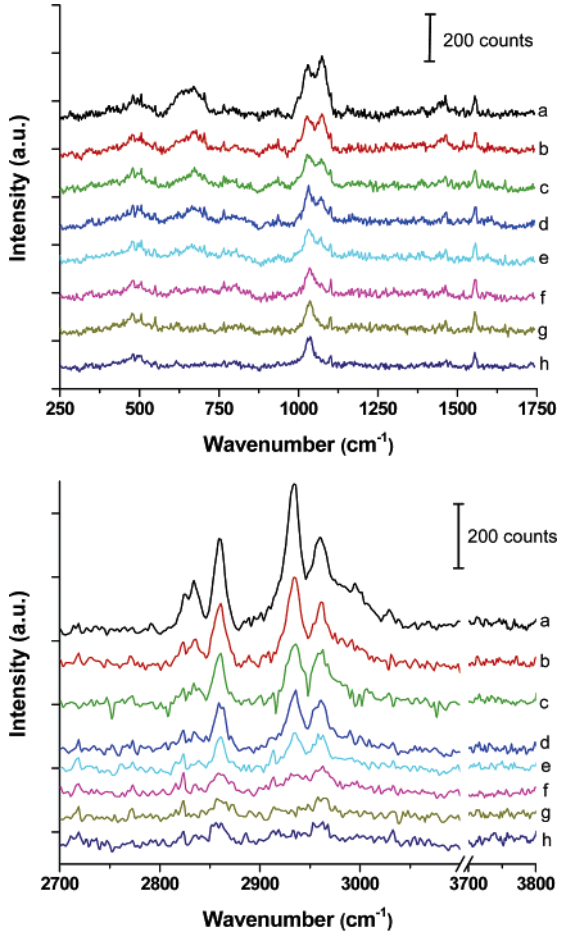

Figure 11. Low and high wavenumber Raman spectra of 3.4V/MCM-48 taken during TPD of adsorbed methanol: (a) 323, (b) 373, (c) 423, (d) 473, (e) 523, (f) 573, (g) 623, and (h) 673 K. Flow rate of He is 30 cm^3 min^{-1}.

calculations have shown similar structures to be stable and likely to be involved in the exchange of O atoms between metal oxo species and silica.[39] The assumption that CH_4 is produced exclusively from $Si-OCH_3$ groups is supported by the Raman spectra taken at temperatures where CH_4 is produced, >550 K, which show that only $Si-OCH_3$ groups remain on the catalyst under these conditions. It is notable that no water is released during TPD, which suggests that V−OH and Si−OH groups do not react to reform V−O−Si bonds under the conditions of a TPD experiment.

Comparison of Figures 12 and 14 shows that up to 550 K the products formed and the shapes of the product peaks observed in TPO and TPD are very similar with only one exception, which is the appearance of H_2O as a product as soon as the TPO experiment is initiated. Since the O_2 used for the experiment is dry and H_2O is not observed in other TPO experiments below 550 K, it is concluded that O_2 induces the release of H_2O from species associated with the catalyst. The shape of the peak for CH_2O is very similar to that observed during TPD, suggesting the processes involved in forming CH_2O during TPO and TPD are identical and do not involve molecular O_2. Figure 18 presents a scheme for rationalizing the appearance of the products formed during TPO. In this figure, the distribution of $V-OCH_3/Si-OH$ and $V-OH/Si-OCH_3$ group pairs is taken to be the same as that for TPD. CH_2O is produced via the identical process shown in Figure 17, and again a portion is taken to escape to the gas phase and a portion undergoes decomposition to CO and H_2. The CO escapes to the gas phase;

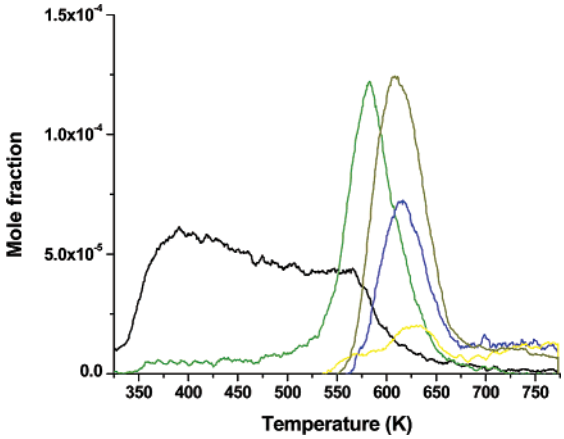

Figure 12. Gas-phase concentrations observed during TPD of methanol adsorbed on 3.4V/MCM-48: methanol, black; formaldehyde, green; carbon monoxide, dark blue; methane, gold; and hydrogen, yellow. Flow rate of He is 30 cm^3 min^{-1}.

however, in contrast to TPD, all of the H_2 is combusted to H_2O. During TPO the $Si-OCH_3$ groups are shown to undergo oxidation to H_2O, CO_2, and small amount of CO. The broad peaks seen at high temperature in Figure 14 are thought to derive from this process. The distribution of reaction products shown in Figure 18 indicates that about two-thirds of the total amount of water formed during TPO can be ascribed to the combustion of H_2 and $Si-OCH_3$. The remaining one-third is thought to be produced by the reaction of vanadyl hydroxyl groups with

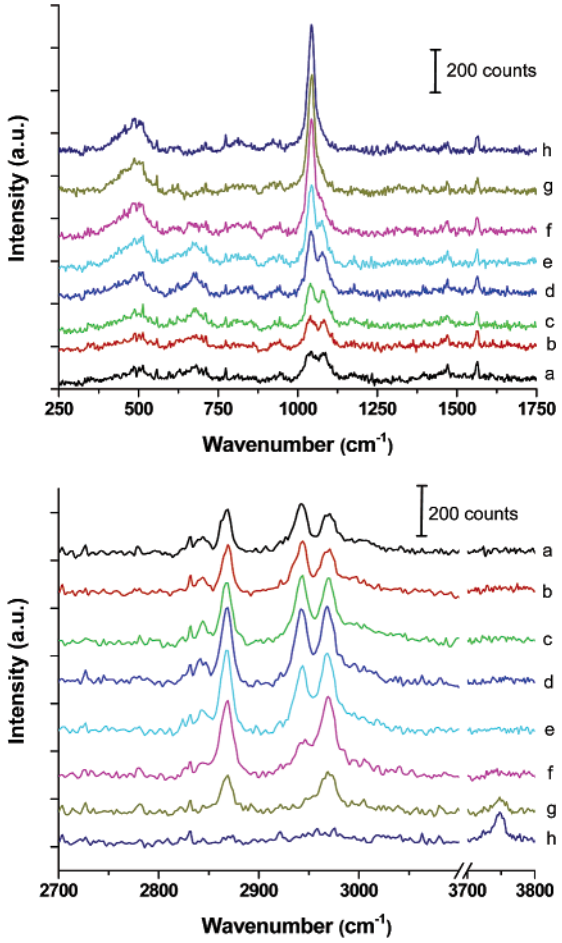

Figure 13. Low and high wavenumber Raman spectra of 3.4V/MCM-48 taken during TPO of adsorbed methanol: (a) 323, (b) 373, (c) 423, (d) 473, (e) 523, (f) 573, (g) 623, and (h) 67 3K. Flow rate of 5%O_2/He is 30 cm^3 min^{-1}.

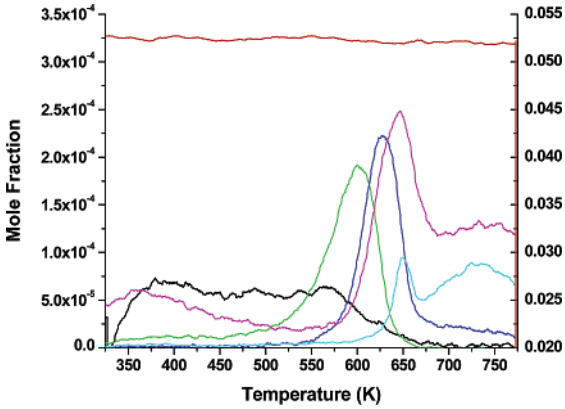

Figure 14. Gas-phase concentrations observed during TPO of methanol adsorbed on 3.4V/MCM-48. Flow rate of 5% O_2/He is 30 cm^3 min^{-1}. Left axis: methanol, black; formaldehyde, green; water, pink; carbon monoxide, dark blue; carbon dioxide, light blue. Right axis: oxygen, red.

silanol groups. It is also possible that the additional H_2O derives from a partial recombination of V−OH and Si−OH groups facilitated by the presence of O_2. This might explain the appearance of H_2O at low temperatures during TPO; however, further work needs to be done to understand how O_2 can facilitate the release of H_2O.

An analysis of the TPRx data presented in Figure 16 shows that up to 625 K, the oxidation of methanol produces CH_2O and H_2O in stoichiometric quantities, consistent with the reaction

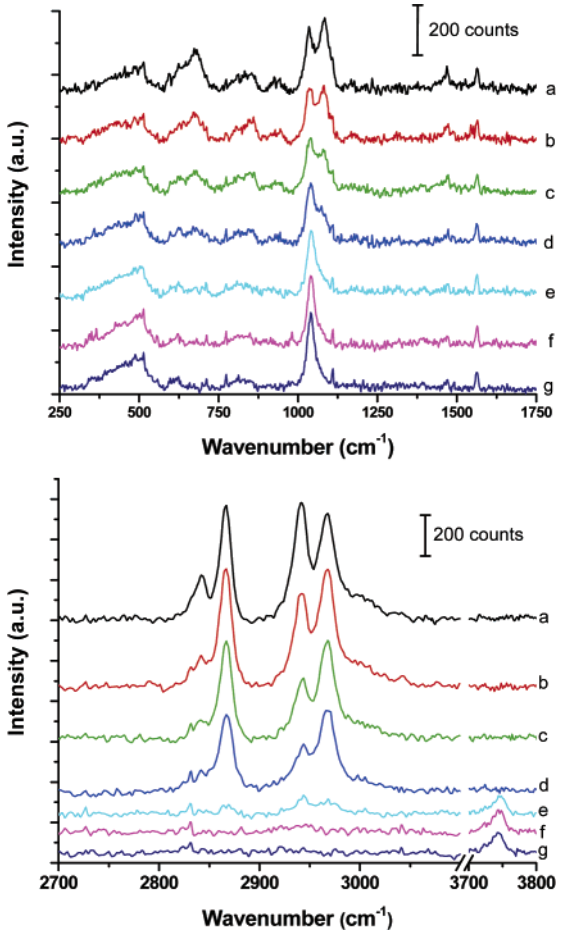

Figure 15. Low and high wavenumber Raman spectra of 3.4V/MCM-48 observed during TPRx in 5%MeOH/7.5%O_2/He flowing at 30 cm^3 min^{-1}: (a) 473, (b) 523, (c) 573, (d) 623, (e) 673, (f) 723, and (g) 773 K.

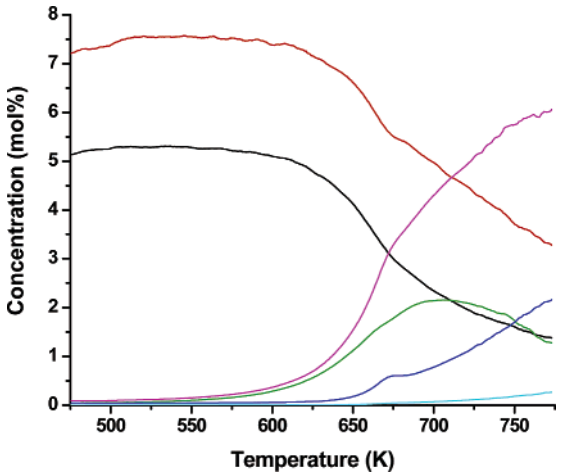

Figure 16. Gas-phase concentrations observed during TPRx of 3.4V/MCM-48 in 5%MeOH/7.5%O_2/He flowing at 30 cm^3 min^{-1}: methanol-black; oxygen, red; formaldehyde, green; water, pink; carbon monoxide, dark blue; and carbon dioxide, light blue.

$CH_3OH + {}^1/_2O_2 \rightarrow CH_2O + H_2O$. The apparent activation energy for this reaction, calculated from an Arrhenius plot of rate of CH_2O formation versus inverse temperature for temperatures between 560 and 650 K, is 23 ± 1 kcal/mol. This value is somewhat larger than the experimental value reported by Deo and Wachs,[5] 19 ± 2.3 kcal/mol, and somewhat smaller than the theoretical value reported by Döbler and Sauer,[38] 27.3 kcal/mol. In the latter work an isolated vanadate species supported

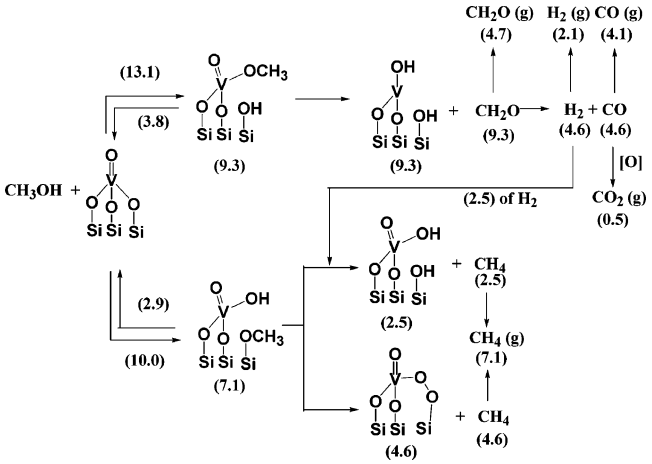

Figure 17. Scheme showing the flow of species and the proposed intermediates for the TPD experiment on 3.4V/MCM-48. Numbers in parentheses under each species are the amount of that species, in μmol, present after each step. The numbers in parentheses near the arrows on the left are the amount of methanol adsorbed and desorbed. The species followed by "(g)" are those that enter the gas phase and are detected experimentally.

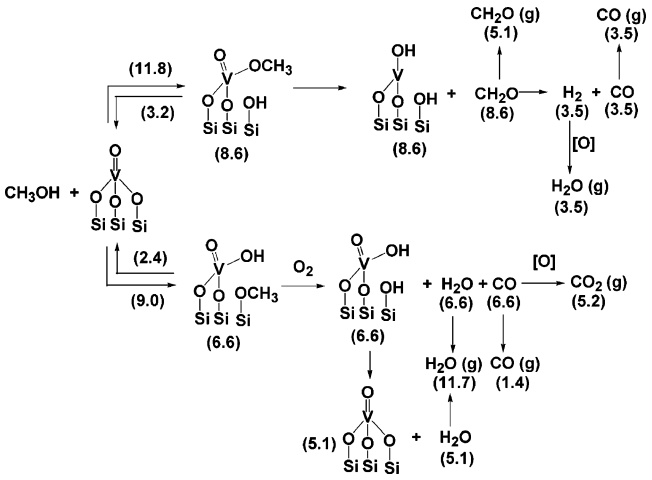

Figure 18. Scheme showing the flow of species and the proposed intermediates for the TPO experiment on 3.4V/MCM-48. Numbers in parentheses under each species are the amount of that species, in μmol, present after each step. The numbers in parentheses near the arrows on the left are the amount of methanol adsorbed and desorbed. The species followed by "(g)" are those that enter the gas phase and are detected experimentally.

on silica was modeled by using density functional theory as a VO_4 group substituted for a $SiO_3(OH)$ group in silsesquioxane. Methanol was found to adsorb by addition across a V−O−Si linkage, leading to the formation of a V−OCH_3/SiOH pair. The rate-limiting step in the formation of CH_2O was found to be the transfer of an H atom from V−OCH_3 to the V═O group.

At higher temperatures, products due to the decomposition of formaldehyde are observed. Above 625 K CO is formed due to the decomposition of CH_2O, and above 675 K CO_2 is formed by combustion of CO. More H_2O is also formed during these reactions, as predicted based on the stoichiometry of the combustion reactions. A check of both the carbon and hydrogen balances shows that they are maintained throughout the entire range of temperatures used in the experiment, indicating that no carbon or hydrogen is deposited onto the catalyst during TPRx.

Conclusions

Raman, XANES, and EXAFS characterization of 3.4V/MCM-48 prepared with a loading of 0.3 V/nm^2 shows that the vanadium is present predominantly as isolated VO_4 units and that there is no evidence for structures containing V−O−V bonds. The VO_4 species have a single V═O bond and are connected to the support via three V−O−Si bonds. Methanol reacts with Si−O−Si bonds present at the surface of MCM-48 to form Si−OCH_3/Si−OH pairs at the level of ∼0.04 pairs/nm^2. On the other hand, methanol reacts reversibly with the V−O−Si bonds to produce V−OCH_3/Si−OH and V−OH/Si−OCH_3 group pairs in roughly equivalent concentrations. The amount of methanol adsorbed is equivalent on a mole to mole basis to the amount of vanadium dispersed on the catalyst, i.e., 0.3 pairs/nm^2. Formaldehyde is formed exclusively from the methyl group of V−OCH_3. Theoretical analyses of this process suggest that this occurs by transfer of an H atom group to the V═O bond of the vanadium surface containing the methoxide group (see Figures 17 and 18). CO is produced by the decomposition of CH_2O at higher temperature. In the presence of O_2, the H_2 produced by the decomposition of CH_2O is oxidized to H_2O. Si−OCH_3 groups are more stable than V−OCH_3 groups. In the absence of O_2, Si−OCH_3 groups undergo hydrogenation to form CH_4, and in the presence of O_2, oxidation of these groups to CO_x ($x = 1, 2$) and H_2O occurs above 650 K. The results of this investigation show that under steady-state reaction conditions, CH_2O is produced as the dominant product of methanol oxidation at temperatures below 650 K with an apparent activation energy of 23 kcal/mol. V−OCH_3 groups serve as the source of CH_2O, which is believed to be formed via the transfer of an H atom from the methyl group of the V−OCH_3 to the V═O group associated with the same V atom. Above ∼650 K, H_2O and CO_2 are formed by the oxidation of H_2 and a part of the CO released by the decomposition of CH_2O, and additionally by the direct oxidation of Si−OCH_3 groups.

Acknowledgment. This work was supported by the Director, Office of Energy Research, Office of Basic Energy Sciences, Chemical Science Division, of the U.S. Department of Energy under Contract No. DE-AC03-76SF00098. Portions of this research were carried out at the Stanford Synchrotron Radiation Laboratory, a national user facility operated by Stanford University on behalf of the U.S. Department of Energy, Office of Basic Energy Sciences. This research was carried out in part at the National Synchrotron Light Source, Brookhaven National Laboratory, which is supported by the U.S. Department of Energy, Division of Materials Sciences and Division of Chemical Sciences, under Contract No. DE-AC02-98CH10886.

References and Notes

(1) Tilley, T. D. *J. Mol. Catal. A*: *Chem.* **2002**, *182*−*183*, 17.
(2) Thomas, J. M. *Top. Catal.* **2001**, *15*, 85.
(3) Volta, J. C. *Top. Catal.* **2001**, *15*, 121.
(4) Grasselli, R. K. *Top. Catal.* **2001**, *15*, 93.
(5) Deo, G.; Wachs, I. E. *J. Catal.* **1994**, *146*, 323.
(6) Baltes, M.; Cassiers, K.; Van Der Voort, P.; Weckhuysen, B. M.; Schoonheydt, R. A.; Vansant, E. F. *J. Catal.* **2001**, *197*, 160.
(7) Lim, S.; Haller, G. L. *Appl. Catal. A* **1999**, *188*, 277.
(8) Gao, X.; Banares, M. A.; Wachs, I. E. *J. Catal.* **1999**, *188*, 325.
(9) Wachs, I. E.; Jehng, J. M.; Deo, G.; Wechkuysen, B. M.; Guliants, V. V.; Benzinger, J. B.; Sundaresan, S. *J. Catal.* **1997**, *170*, 75.
(10) Burcham, L. J.; Deo, G.; Gao, X.; Wachs, I. E. *Top. Catal.* **2000**, *11/12*, 85.
(11) Olthof, B.; Khodakov, J.; Bell, A. T.; Iglesia, E. *J. Phys. Chem. B* **2000**, *104*, 1516.
(12) Wang, C.-B.; Deo, G.; Wachs, I. E. *J. Catal.* **1998**, *178*, 640.

(13) Zhang, Q.; Yang, W.; Wang, X.; Wang, Y.; Shishido, T.; Takehira, K. *Microporous Mesporous Mater.* **2005**, *77*, 223.
(14) Zhang, S. G.; Higashimoto, S.; Yamashita, H.; Anpo, M. *J. Phys. Chem. B* **1998**, *102*, 5590.
(15) Burcham, L. J.; Wachs, I. E. *Catal. Today* **1999**, *49*, 467.
(16) Khaliullin, R.; Bell, A. T. *J. Phys. Chem. B* **2002**, *106*, 7832.
(17) Morey, M. S.; Davison, A.; Stucky, G. D. *J. Porous Mat.* **1998**, *5*, 195.
(18) Huo, Q.; Margolese, D. E.; Stucky, G. D. *Chem. Mater.* **1996**, *8*, 1147.
(19) Alami, E.; Beinert, G.; Marie, P.; Zana, R. *Langmuir* **1993**, *9*, 1465.
(20) Baltes, M.; Van Der Voort, P.; Collart, O.; Vansant, E. F. *J. Porous Mater.* **1998**, *5*, 317.
(21) Barrett, E. P.; Joyner, L. G.; Halenda, P. P. *J. Am. Chem. Soc.* **1951**, *73*, 373.
(22) Jentoft, R. E.; Deutsch, S. E.; Gates, B. C. *Rev. Sci. Instrum.* **1996**, *67*, 2111.
(23) Newville, M. *J. Synchrotron Radiat.* **2001**, *8*, 322.
(24) Ravel, B.; Newville, M. *J. Synchrotron Radiat.* **2005**, *12*, 537.
(25) Wachs, I. E.; Weckhuysen, B. M. *Appl. Catal. A* **1997**, *157*, 67.
(26) Xie, S.; Iglesia, E.; Bell, A. T. *Langmuir* **2000**, *16*, 7162.
(27) Pasquarello, A.; Car, R. *Phys. Rev. Lett.* **1998**, *80*, 5145.
(28) Wong, J.; Lytle, F. W.; Messmer, R. P.; Maylotte, D. H. *Phys. Rev. B* **1984**, *30*, 5596.
(29) Soares, A. P. V.; Portela, M. F.; Kiennemann, A.; Hilaire, L. *Chem. Eng. Sci.* **2003**, *58*, 1315.
(30) Ankudinov, A. L.; Bouldin, C.; Rehr, J. J.; Sims, J.; Hung, H. *Phys. Rev. B* **2002**, *65*, 104107.
(31) Tanaka, T.; Yamashita, H.; Tsuchitani, R.; Funabiki, T.; Yoshida, S. *J. Chem. Soc., Faraday Trans. 1* **1988**, *84*, 2987.
(32) Li, W.; Willey, R. J. *J. Non-Cryst. Solids* **1997**, *212*, 243.
(33) Gao, X.; Bare, S. R.; Weckhuysen, B. M.; Wachs, I. E. *J. Phys. Chem. B* **1998**, *102*, 10842.
(34) Busca, G.; Elmi, A. S.; Forzatti, P. *J. Phys. Chem.* **1987**, *91*, 5263.
(35) Falk, M.; Whalley, E. *J. Chem. Phys.* **1961**, *34*, 1554.
(36) Xie, S.; Iglesia, E; Bell, A. T. *J. Phys. Chem. B* **2001**, *105*, 5144.
(37) Feng, T.; Vohs, J. M. *J. Phys. Chem. B* **2005**, *109*, 2120.
(38) Dobler, J.; Pritzsche, M.; Sauer, J. *J. Am. Chem. Soc.* **2005**, *127*, 10861.
(39) Chempath, S.; Bell, A. T. unpublished results.